HAWAII 167 and Q0059-2735: Heavily Dust-Enshrouded Young QSOs

E. Egami[1,2]

Institute for Astronomy, University of Hawaii, 2680 Woodlawn Drive, Honolulu, HI 96822

egami@mpe-garching.mpg.de

F. Iwamuro, T. Maihara, and S. Oya

Department of Physics, Kyoto University, Kitashirakawa, Kyoto 606-01, Japan

iwamuro@cr.scphys.kyoto-u.ac.jp, maihara@cr.scphys.kyoto-u.ac.jp,

oya@cr.scphys.kyoto-u.ac.jp

and

L. L. Cowie

Institute for Astronomy, University of Hawaii, 2680 Woodlawn Drive, Honolulu, HI 96822

cowie@ifa.hawaii.edu

Received _____; accepted _____

[1]Visiting Astronomer, United Kingdom Infrared Telescope, operated by the Royal Observatory Edinburgh for the UK Science and Engineering Research Council.

[2]Current address: Max-Planck-Institut für extraterrestrische Physik, Postfach 1603, 85740 Garching, Germany

ABSTRACT

Using the OH-airglow suppressor spectrograph at the University of Hawaii 2.2m telescope and the CGS4 spectrometer at the United Kingdom Infrared Telescope, we have found exceptionally large Balmer decrements in two unusual high-z QSOs, Hawaii 167 ($z = 2.36$, Hα/H$\beta = 13$) and Q0059-2735 ($z = 1.59$, Hα/H$\beta = 7.6$), the latter being a so-called low-ionization broad absorption line QSO (BALQSO). We argue that these objects are young QSOs heavily enshrouded by dust. In fact, the internal reddening might be so large as to completely extinguish the QSO light in the restframe UV, allowing us to see the underlying stellar population. Our possible detection of the 4000 Å break in Hawaii 167 supports this idea. Its small amplitude indicates a very young age for the population, ~ 15 Myrs. To explain the properties of these QSOs, we propose a model in which a young QSO is surrounded by a shell of young massive stars mixed with significant amounts of dust. We predict that as the QSO emerges from this dust cocoon, it will eventually take on the appearance of a normal BALQSO.

Subject headings: quasars: emission lines — galaxies: starburst — dust, extinction — galaxies: individual (Hawaii 167) — quasars: individual (Q0059-2735)

1. INTRODUCTION

In the Hawaii deep K-band survey (Cowie et al. 1994a; Songaila et al. 1994), one extraordinary object was found at a redshift[3]of 2.36, the highest by far in the sample. This object, named Hawaii 167, has strange characteristics: its high redshift, compact morphology, and broad ($\sim$ 5000 km s^{-1}) Balmer emission lines are sure signs of this object's being a QSO while its restframe UV spectrum resembles those of starburst galaxies, showing strong metal absorption lines with no obvious emission features (Cowie et al. 1994b). Cowie et al. (1994b) suggested that Hawaii 167 was either a very exotic broad absorption line QSO (BALQSO), a starburst galaxy, or most probably a mixture of both. If Hawaii 167 is in any way related to starbursts, it may be of considerable importance: the small area coverage of the survey ($\sim$ 77 arcmin^{-2}) suggests that this type of object might in fact be quite common in faint near-IR samples.

The key to understanding Hawaii 167 may lie in the QSO called Q0059-2735 (Hazard et al. 1987), the only previously known object with similar characteristics. This object is the most extreme member of the low-ionization BALQSOs (also often called Mg II BALQSOs) comprising $\sim$ 15% of BALQSOs, which themselves represent $\sim$ 10% of all QSOs (Weymann et al. 1991). This class of QSOs shows broad absorption lines (BALs) of low-ionization ions (Mg II, Al III) as well as those of the high-ionization species (C IV, Si IV) regularly seen in BALQSOs. What separates low-ionization BALQSOs from the normal BALQSOs seems to be their richness in dust: they are known to be more common in IRAS-selected samples (Low et al. 1989), and their UV continuum shows signs of moderate reddening (Sprayberry & Foltz 1992). Also, the absence or the extreme weakness of [O III] in these objects can be understood if dust is preventing ionizing radiation from reaching the outer low-density

[3]The redshift was originally reported as 2.35, but our reanalysis of the Hα line indicates that it is closer to 2.36.

regions where the formation of the forbidden line is possible (Boroson & Meyers 1992). Voit et al. (1993) suggested that low-ionization BALQSOs are probably "young quasars in the act of casting off their cocoons of gas and dust," which implies some kind of connection between these objects and the ultraluminous IRAS galaxies (Sanders et al. 1988). Indeed, one of the ultraluminous IRAS galaxies, IRAS 07598+6508, was found to be a low-ionization BALQSO (Lipari 1994).

As already mentioned, one interpretation for Hawaii 167 put forth by Cowie et al. (1994b) was that Hawaii 167 is a mixture of both a QSO and a starburst galaxy: its internal reddening is so large that its QSO light, dominating the restframe optical, is completely extinguished in the restframe UV, leaving only the light of the surrounding starbursting galaxy. This idea is supported by the lack of any UV broad emission lines (BELs), and the large Balmer decrement (> 8) inferred from the non-detection of Hβ. In this paper, we will investigate this possibility by examining the near-IR spectra of Hawaii 167 and Q0059-2735, using the Balmer decrement as an indicator of internal reddening.

2. THE DATA

The K-band (Hα) spectrum of Hawaii 167 was taken on the night of 1993 December 21 using the CGS4 spectrometer (Mountain et al. 1990) at the United Kingdom Infrared Telescope (UKIRT) on Mauna Kea. The 75 line mm^{-1} grating used in first order gave a resolving power, R, of ~ 340 with a $3''$ (1 pixel) slit. An adequate sampling was achieved by shifting the detector over 2 pixels in 4 steps in the wavelength direction. The integration time at each detector position was 30 seconds, and the total integration time was 28 minutes. This data was summarized in Cowie et al. (1994b).

The J-band ([O II]) and H-band (Hβ) spectra of Hawaii 167 were taken on the nights

of 1994 October 24–30 using the OH-airglow suppressor spectrograph (Iwamuro et al. 1994) at the University of Hawaii 2.2 m telescope on Mauna Kea. This spectrograph produces both J- and H-band spectra simultaneously with R $\sim$ 100. With a 1.5″ wide slit, this spectrograph first projects J- and H-band spectra on a mask mirror with R $\sim$ 5500. The mask mirror has narrow black (non-reflecting) stripes on the positions of the OH sky lines, and therefore removes the contribution from these lines upon the reflection of the light. This light is subsequently recombined to produce final low-resolution spectra (R $\sim$ 100) with a sky background reduced by a factor of $\sim$ 20. The total integration time was 11 hours and 44 minutes (8 minutes $\times$ 88 frames).

Spectra of Q0059-2735 were taken in the H band (Hα) and J band (Hβ) on the nights of 1994 October 8 and 9, respectively, using the CGS4 spectrometer at UKIRT. This object was observed as a filler during the observing run allocated for the follow-up spectroscopy of a $z > 4$ galaxy survey (Egami 1995). The 75 line mm^{-1} grating was used in first order in the H band and in second order in the J band. With a 3″ (2 pixels) slit, this gave R $\sim$ 250 (H) and $\sim$ 380 (J). The detector was shifted over 2 pixels in 6 steps. The integration time at each position was 60 seconds, and the total integration time was 36 minutes in each band.

The reduced spectra are shown in Fig. 1 (Hawaii 167) and Fig. 2 (Q0059-2735). The measured line parameters are summarized in Table 1. These measurements are based on gaussian profile fitting, and the derived fits are drawn in the figures as the thick solid lines. We have adopted the fitting procedure of Baker et al. (1994) so that we can compare our Balmer decrement measurements with theirs. The quoted errors are internal fitting errors (1 σ) and determined by performing one hundred Monte Carlo simulations. By comparing with the broad-band magnitudes listed in Cowie et al. (1994b) (the horizontal dash-dot lines in the figures), we estimate the photometric accuracy to be 10–20% after the contribution from the emission lines is taken into account. The broad-band J magnitude of Q0059-2735

seems to be significantly higher than the continuum level of our spectrum, but we think this offset could be real. There are complexes of Fe II emission lines just outside our spectral band in both directions, and these Fe II complexes have been found to be extremely strong in ultraluminous IRAS galaxies (Lipari, Terlevich, & Macchetto 1993) and high-z QSOs (Hill, Thompson, & Elston 1993). These Fe II emission complexes are within the passband of the J band, and might be boosting the broad-band flux level. In the case of Q0059-2735, two gaussians were used simultaneously for the Hα to obtain a good fit, and for the Hβ we mirror-reflected the left half of the line and then fitted a gaussian in order to avoid the contamination from Fe II emission, whose presence is clearly seen in the figure on the right side of the line. In the case of Hawaii 167, we do not think that the peak near 5007 Å is a real feature because its width was found to be smaller than the instrumental profile; it also lies very close to the edge of the spectrum, reinforcing the possibility that this feature is an artifact.

3. DISCUSSION

The values of the Balmer decrements found for these QSOs are exceptionally large. Although the Balmer decrements of most QSOs are known to be significantly larger than 2.87, which is the case B recombination value at T = 10^4 K, their typical range seems to be 3 – 6 (Baker et al. 1994). This is still much smaller than the values for Hawaii 167 (13) and Q0059-2735 (7.6). Considering the mounting evidence for the low-ionization BALQSOs being dust rich, it seems natural to think that the presently measured large Balmer decrements are a result of heavy reddening by internal dust extinction.

The amounts of internal reddening inferred from the Balmer decrements are very significant. For example, if we assume Hα/H$\beta \leq 6$ for normal QSOs, we obtain $E(B-V) \geq 0.19$ and 0.54 for Q0059-2735 and Hawaii 167, respectively, after the foreground Galactic red-

dening ($E(B-V) = 0.02$ for Q0059-2735 and 0.14 for Hawaii 167) is taken into account. The actual values may be closer to $E(B-V) = 0.35$ and 0.70, corresponding to an intrinsic Balmer decrement of 5. This means that these QSOs must be heavily enshrouded by dust — for an extinction law similar to that in our galaxy, these values of the color excess correspond to A(1500 Å) ~ 3 and 6. If the amount of extinction is in fact of such magnitude, the consequence will be profound: this much dust is capable of completely extinguishing the light from the QSO in the restframe UV, allowing us to see the underlying stellar population in high redshift QSOs for the first time.

Given a high extinction to the QSO, the origin of the UV continuum light is unclear. It becomes especially puzzling if we consider the fact that the spectra of these objects are as flat as those of normal QSOs ($f_\nu \propto \nu^{-1}$, see Fig. 3). In other words, *these objects have simply too much UV light for their Balmer decrement values.* In what follows, we will try to explain the origin of the observed UV light in terms of three different hypotheses: reddened QSO light, scattered QSO light, and star light from the surrounding stellar population.

The main requirement for these models is to explain the two salient characteristics of these QSOs: the large Balmer decrements and the small equivalent widths of the BELs, especially those of Mg II (Cowie et al. 1994b) and Hβ (Table 1). We do not include the high-ionization BELs here because their small equivalent widths could be explained by other mechanisms. For example, large blueshifts of high-ionization BELs, often seen in QSOs, will result in the destruction of these lines by the broad absorption line region (BALR). In the case of Q0059-2735, a blue shift of ~ 700 km s^{-1} was suggested for the C IV BEL by Wampler, Chugai, & Petitjean (1995). On the other hand, if most high-ionization BELs actually come from the BALR as suggested by Turnshek (1984), dust in the BALR, provided that it is mixed with the ions, could preferentially destroy resonance-line photons, which include most of the high-ionization BELs (Voit, Weymann, & Korista 1993). Note, however, that neither

of these explanations would work with the Mg II BEL: a low-ionization BEL such as Mg II is very unlikely to have a large blueshift, and also the Mg II BEL probably cannot form in the BALR (Turnshek et al. 1984).

In the following, we will examine in turn the three hypotheses proposed above. In order to estimate the contribution of the QSO light, we assume its intrinsic spectrum to be: (1) $f_\nu \propto \nu^{-1}$, (2) Hα/H$\beta = 5$.

3.1. The Reddened-QSO-light Hypothesis

The reddened-QSO-light hypothesis explains the UV spectrum simply as a reddened QSO continuum. The upper plot of Fig. 3 shows that if the flat continuum spectrum from a QSO (A) is reddened with the SMC extinction law (Prévot et al. 1984) and $E(B-V) = 0.08$, it can more or less reproduce the overall shape of the observed spectrum of Hawaii 167 (B). This combination of the SMC extinction law with a moderate amount of reddening was used to explain the SEDs of low-ionization BALQSOs by Sprayberry & Foltz (1992). This might also be the case with Q0059-2735, but it is hard to judge only from the broad-band UV measurements we have (lower plot).

The problem with this explanation is its inevitable conclusion that the continuum suffers much less reddening than the broad Balmer lines ($E(B-V) = 0.08$ vs. 0.70 for Hawaii 167). It is almost certain that the dust responsible for the reddening does not exist in the broad emission line region (BELR): the space between the BEL clouds is exposed to continuum radiation too strong for the existence of dust while the BEL clouds themselves seem to be free from internal dust, showing no reduction of resonance BELs (e.g., C IV) with respect to non-resonance BELs (e.g., C III]) (Netzer 1990). The theoretical calculation by Laor & Draine (1993) also indicates that the dust cannot probably exist in the BELR. This means

that the reddening must take place outside the BELR, and probably within or behind the BALR where dust is protected from the strong radiation. However, it is very difficult to imagine that such a dust distribution could affect the BEL photons and the continuum photons differently, causing a different amount of reddening for each component. Therefore in this case, we need to assume that the large Balmer decrements are intrinsic to these QSOs, and that the actual reddening with the BELs is as small as that of the continuum. The problem is that it is unclear whether such a large deviation of the intrinsic Balmer decrements is feasible. Also, this still cannot explain the small equivalent widths of Mg II and Hβ because reddening by itself cannot change the equivalent widths of the BELs.

3.2. The Scattered-QSO-light Hypothesis

The scattered-QSO-light hypothesis would explain the UV light as scattered light from the QSO while maintaining the same amount of reddening for both the BELs and the continuum. In the Fig. 4, the flat QSO spectra (A and C) are reddened by the SMC extinction law with color excesses derived from the Balmer decrements, assuming its intrinsic value of 5. These reddened QSO spectra are then scaled such that they would give the observed flux at the Hα wavelength (B and D). Note that such a scaling will minimize the amount of the UV light which must be explained as scattered light. With this procedure, the contribution of the reddened QSO light to the observed flux at Mg II, Hβ, and Hα is estimated to be 13%, 58%, and 100% for Hawaii 167, and 24%, 88%, and 100% for Q0059-2735, respectively. In other words, most of the UV light must be scattered light. The contribution from the scattered light component must then be such that if combined with the reddened continuum, it will produce an apparent spectrum which matches a flat spectrum with moderate reddening.

The problem with this model is the extreme efficiency of scattering required to produce the observed UV spectrum. This is immediately clear from the fact that the observed spectra

of these objects are as flat as those of normal QSOs. In the case of Hawaii 167, the observed flux at 2000 Å is still 35 % of the original power-law value. Although such an efficiency is possible for a single-scattering process, it is still impossibly high for a process involving a large number of scatterings, which is undoubtedly the case for this heavily reddened QSO. If we assume that each photon moves outward by random walks, it must go through on the order of $(\tau_{2000})^2$ scatterings, where τ_{2000} is the optical depth at 2000 Å. Since A(2000 Å) = 6.6 for $E(B-V) = 0.70$ and $R = 3.1$ with the SMC extinction law, τ_{2000} is ~ 6.1. Therefore, each photon must be scattered ~ 37 $(= 6.1^2)$ times before escaping outside. In order to achieve an effective efficiency of 35% after this many scatterings, we need a dust albedo of 0.97 at 2000 Å, which is quite unlikely. Although it is certain that there exists some amount of scattered QSO light, there is probably not so much as to explain all the UV light seen. This model also cannot explain the small equivalent widths of Mg II and Hβ because scattering by itself cannot change the equivalent widths of the BELs.

So far, we have seen that neither the reddened-QSO-light hypothesis nor the scattered-QSO-light hypothesis can explain the nature of these objects very well. The main problem is the mismatch between the large Balmer decrements and the flat spectra of these objects. Furthermore, neither hypothesis can explain the observed small equivalent widths of the Mg II and Hβ BELs. For these models to be true, we need to assume that either their small equivalent widths are intrinsic to the QSOs, or that there is some mechanism at work which preferentially destroys the BEL photons. However, a more natural explanation would be to invoke another component of the light which is diluting the QSO light. This leads to the possibility that the UV spectra of these QSOs are dominated by the light from their surrounding stellar populations. We now examine this hypothesis.

3.3. The Star-light Hypothesis

Direct support for the star-light hypothesis comes from the suggested detection of the 4000 Å break in the spectrum of Hawaii 167. Although the shape of the break is ambiguous, there is clearly an offset in the continuum level between the J and H bands of Hawaii 167 (Fig. 1). In Fig. 4, we tried to fit this 4000 Å break with the isochrone-synthesis model by Bruzual and Charlot (1993) after subtracting the reddened-QSO-light model C from the observed spectrum. One thing is immediately obvious: the small 4000 Å break is incompatible with the large drop of flux around 2000 Å. A young stellar population consistent with the small 4000 Å break produces too much UV light (A) while an older population matching the flux drop at 2000 Å becomes too red in the UV–optical color (B). Here, we used the instantaneous starburst model to accelerate the depression of the UV light as much as possible, but it was still not fast enough to produce these two features simultaneously. One way to get around this problem is to introduce a moderate amount of reddening. An extremely young flat-spectrum population (D) reddened with the SMC extinction law and $E(B-V) = 0.23$ can more or less reproduce the observed spectrum (E). Although the fit is not perfect, it is probably acceptable if we consider the various uncertainties such as the geometry of the dust distribution and the properties of the dust particles, and in any case as good as the line (B) in Fig. 3. Fig. 5 shows the comparison between the model (E) and the actual near-IR spectra shown in Fig. 1.

A caveat to this explanation is its implicit but unavoidable conclusion that the BALs seen in these QSOs have nothing to do with the BALQSO phenomena, which we usually associate with the activities of the QSO itself, but are features in the starbursting galaxy surrounding the QSO. Recall our argument that the reddening of the QSO continuum and the BELs should take place within or behind the BALR where dust is protected from the strong radiation (see Section 3.1). If this is the case, whatever is lying inside the BALR must

be as reddened as the continuum and the BELs. Since the stellar UV continuum seems to suffer much milder reddening, this will put the position of the stellar population outside the BALR. However, such a configuration obviously cannot produce the BALs in the stellar UV continuum. Therefore, we need to think that the BALs seen in these QSOs are produced by this same stellar population. In the case of Hawaii 167, the widths of the BALs are somewhat narrower than usual ($\sim$ 1500 (Mg II) – 4500 (Si IV) km s^{-1}), and therefore they might be explained as stellar absorption lines produced by a starbursting population (Cowie et al. 1994b); The BALs seen in Q0059-2735, on the other hand, show outflow velocities as high as 20000 km s^{-1}, so the ejecta of supernova explosions are the only possible explanation.

This model, though plausible, cannot help but look somewhat arbitrary in that it devises yet another mechanism for producing the BALs. Here, we suggest that it is possible to construct a more simple and coherent model of these QSOs and the BALQSO phenomena in general in the framework of the dusty nuclear-starburst model (Lipari, Colina, & Macchetto 1994; Lipari 1994). Suppose that in the nuclear region of these galaxies, the central BELR is surrounded by a shell of starbursting stellar population mixed with dust. The BELs will show large amounts of reddening because the BEL photons must transverse this dusty shell. The stellar continuum, on the other hand, will show much smaller amounts of reddening partly because the composite light is dominated by stars with smaller extinction, and partly because scattered light compensates for reddening by extinction (Witt et al. 1992). The BALs are probably produced in this shell as a result of supernova explosions. The ejecta of these explosions will preferentially extend outward and show blueshifts because of the smaller ambient density toward that direction. We see these outflowing gas clouds against the stellar continuum or the QSO continuum in the case of normal BALQSOs, recognizing them as the BALs.

This model could also explain the main characteristics of the low-ionization BALQSOs

(Lipari, Colina, & Macchetto 1994; Lipari 1994). For example, such dusty environments will prevent ionizing photons from escaping to the outer low-density regions where the formation of [O III] is possible, explaining the absence or the extreme weakness of this line. Also, supernova explosions are a natural way to explain the formation of Fe, whose emission and absorption lines are found to be abnormally strong (Hazard et al. 1987; Wampler, Chugai, & Petitjean 1995; see also Fig. 2). We further speculate that this shielding of ionizing radiation also allows the existence of low-ionization ions such as Mg II and Al III, whose absorption lines characterize the spectra of these QSOs.

These dust-enshrouded QSOs will eventually emerge from the dust cocoons once the dust in the surrounding shell is cleared away by various energetic processes such as radiation pressure from the QSOs, supernova explosions, and stellar winds (Sanders et al. 1988; Lipari, Colina, & Macchetto 1994; Lipari 1994). If this happens, all the characteristics of these QSOs mentioned above will go away: the [O III] emission will become stronger because the ionizing photons start to reach the outer low-density region; the low-ionization BALs will disappear because these ions will be more highly ionized; and the emission and absorption by Fe II and Fe III will weaken because these ions will also move to higher ionization stages. The resultant objects will be normal-looking BALQSOs. Therefore, if this model is correct, we expect that the low-ionization BALQSOs and the normal BALQSOs form an evolutionary sequence. Although the argument so far does not require the geometry of the standard AGN Unified Theories, in this framework such a transition might be identified as the development of ionization cones while we are looking at these objects pole-on.

4. CONCLUSIONS

Although any conclusion drawn from such a small data set is necessarily tentative, at this point we think that the star-light hypothesis is the most likely explanation for the spectra

of these QSOs. It is very difficult to imagine that the intrinsic Balmer decrement could be close to, or even larger than 10 as in the case for the reddened-QSO-light hypothesis; nor is it easy to imagine that any dust grains could have UV albedos close to unity as in the case for the scattered-QSO-light hypothesis. Furthermore, neither of these could explain the small observed equivalent widths of the Mg II and Hβ BELs. Therefore, we conclude that these objects are in fact heavily dust-enshrouded young QSOs whose internal reddening is so large as to completely extinguish the QSO light in the restframe UV, allowing us to see the underlying stellar population.

A possible counter argument to this explanation, nevertheless, is to attribute the large Balmer decrements and the small equivalent widths to the scatter in the intrinsic QSO properties. This argument is especially strong for Q0059-2735, whose Balmer decrement and Hβ equivalent width are deviant but might still be within the range of their natural distribution, which itself has a large scatter. Our response to such an argument is that low-ionization BALQSOs are very likely to be dusty from other lines of evidence (see Introduction), and therefore it is very natural to explain the peculiar properties of these objects as the effect of dust. Probably most of the low-ionization BALQSOs discovered so far are not as heavily reddened as the two objects studied here because the determination of the low internal reddening by Sprayberry & Foltz (1992) stems not only from the continuum shape but also from the emission line strength. Our claim, however, is that there are objects which are extreme versions of these optically selected low-ionization BALQSOs, and they are probably as dusty as the ultraluminous IRAS galaxies. The identification of one of the ultraluminous IRAS galaxies, PC07598+6508, as a low-ionization BALQSO (Lipari 1994) strongly supports this idea. In this sense, these two classes of objects may well be the same things looked at from different angles or at different times.

A model of a young QSO surrounded by a shell of starbursting population mixed with

dust seems to explain (at least qualitatively) the main characteristics of these QSOs, and possibly suggest the evolutionary connection between the low-ionization BALQSOs and normal BALQSOs. This starburst in the shell surrounding a QSO could be identified as spheroid formation (Cowie et al. 1994b; Kormendy & Sanders 1992) though this is a speculative guess at this point. This model of course has its own problems, and we mention a few here: First, it is unclear whether we could really explain the BALQSO phenomena with supernova explosions in this surrounding shell. Second, a great deal of fine-tuning seems to be required if we are to produce an almost perfectly power-law SED out of two completely separate light components, a QSO and its underlying stellar population. Finally, it is uncertain whether the use of the Bruzual-Charlot model is justified for these objects. The starburst might be limited to a class of massive stars within a small mass range; also, the light from supernovae might be dominating the SEDs.

We also mention another rather technical problem: that is, the assessment of effects due to Fe II emission features. It is known that this type of QSO shows strong Fe II emission, and that these features are especially conspicuous around Hβ. Therefore, it is possible that the small equivalent width of Hβ is simply due to a large contribution of Fe II emission to the continuum. Also, our measurement of the 4000 Å break amplitude might be affected by the Fe II emission features. Although these effects are potentially serious, we are not able to assess the effects of Fe II emission here because our limited spectral coverage and resolution prevent us from performing detailed modelling of Fe II emission features.

Despite the various uncertainties, these objects present two very interesting possibilities: that is, 1) heavy internal reddening of QSOs could result in a separation of their stellar light and AGN light in spectral space, and 2) if such heavily reddened QSOs exist at high redshifts, they could easily have escaped our detection until now.

The first point leads us to the possibility that we may be able to study the underlying

stellar populations of QSOs by using this type of object. In this paper, we have presented an example of such analyses, which suggests that the stellar population in Hawaii 167 looks very young, probably around 15 Myrs old if we take the fit of the Bruzual-Charlot model at its face value. The great importance of such a spectral analysis is that we do not have to spatially resolve the QSO: at high redshifts where such a spatial separation becomes difficult, spectroscopic studies of this class of QSOs may be the only way to understand what high-z QSOs really are.

Regarding the second point, if this type of object exists in significant numbers, it is very likely that many of them would not have been picked up in the previous optical surveys due to their faint UV continuum and absence of strong UV emission lines. In fact, Hawaii 167-like objects could be completely dark in the observer's optical band if starbursts have not started in the host galaxy. This implies that there might be a whole population of dust-enshrouded young QSOs at high redshifts which has so far eluded our detection. We were able to identify Hawaii 167 simply because it has barely enough UV continuum for our optical spectroscopy with a 4-m class telescope, and this might explain the flatness of Hawaii 167's SED as a selection effect. In any case, if these objects are in fact young QSOs emerging from their dust cocoons, they are probably much more abundant at $z > 2$, where the comoving space density of QSOs is rapidly increasing. The redshift of Hawaii 167 is indeed just above 2. Wide-field sensitive near-IR surveys should eventually tell us if such a population of objects exists.

We thank S. Charlot for providing the isochrone synthesis model, and E. M. Hu for helpful comments on the manuscript. This work was partly supported by the Grant-in-Aid of the Ministry of Education, Japan (07044080).

REFERENCES

Baker, A. C., Carswell, R. F., Bailey, J. A., Espey, B. R., Smith, M. G., & Ward, M. J. 1994, MNRAS, 270, 575

Boroson, T. A., & Meyers, K. A. 1992, ApJ, 397, 442

Bruzual A., G., & Charlot, S. 1993, ApJ, 405, 538

Cowie, L. L., Gardner, J. P., Hu, E. M., Songaila, A., Hodapp, K.-W., & Wainscoat, R. J. 1994a, ApJ, 434, 114

Cowie, L. L., Songaila, A., Hu, E. M., Egami, E., Huang, J.-S., Pickles, A. J., Ridgway, S. E., & Wainscoat, R. J. 1994b, ApJ, 432, L83

Egami, E. 1995, in Wide Field Spectroscopy and the Distant Universe (The 35th Herstmonceux Conference), ed. S. J. Maddox & A. Aragón-Salamanca (Singapore: World Scientific), 380

Hazard, C., McMahon, R. G., Webb, J. K., & Morton, D. C. 1987, ApJ, 323, 263

Hill, G. J., Thompson, K. L., & Elston, R. 1993, ApJ, 414, L1

Iwamuro, F., Maihara, T., Ohya, S., Tsukamoto, H., Hall, D. N. B., Cowie, L. L., Tokunaga, A. T., & Pickles, A. J. 1994, PASJ, 46, 515

Kormendy, J., & Sanders, D. B. 1992, ApJ, 390, L53

Laor, A., & Draine, B. T. 1993, ApJ, 402, 441

Lipari, S., Terlevich, R., & Macchetto, F. 1993, ApJ, 406, 451

Lipari, S., Colina, L., & Macchetto, F. 1994, ApJ, 427, 174

Lipari, S. 1994, ApJ, 436, 102

Low, F. J., Cutri, R. M., Kleinmann, S. G., & Huchra, J. P. 1989, ApJ, 340, L1

Mountain, C. M., Robertson, D. J., Lee, T. J., & Wade R. 1990, Instrumentation in Astronomy VII, ed. D. L. Crawford (Proc. SPIE, 1235), 25

Netzer, H. 1990, in Active Galactic Nuclei (Saas-Fee Advanced Course 20), ed. T. J.-L. Courvoisier & M. Mayor (Berlin: Springer-Verlag), 57

Prévot, M. L., Lequeux, J., Maurice, E., Prévot, L., & Rocca-Volmerange, B. 1984, A&A, 132, 389

Sanders, D. B., Soifer, B. T., Elias, J. H., Madore, B. F., Matthews, K., Neugebauer, G., & Scoville, N. Z. 1988, ApJ, 325, 74

Savage, B. D., & Mathis, J. S. 1979, ARA&A, 17, 73

Songaila, A., Cowie, L. L., Hu, E. M., & Gardner, J. P. 1994, ApJS, 94, 461

Sprayberry, D., & Foltz, C. B. 1992 ApJ, 390, 39

Turnshek, D. A., Weymann, R. J., Carswell, R. F., & Smith, M. G. 1984, ApJ, 277, 51

Turnshek, D. A. 1984, ApJ, 278, L87

Voit, G. M., Weymann, R. J., & Korista, K. T. 1993, ApJ, 413, 95

Wampler, E. J., Chugai, N. N., & Petitjean, P. 1995, ApJ, 443, 586

Weymann, R. J., Morris, S. L., Foltz, C. B., & Hewett, P. C. 1991, ApJ, 373, 23

Witt, A. N., Thronson, H. A. Jr., & Capuano, J. M. Jr. 1992, ApJ, 393, 6113

This manuscript was prepared with the AAS LaTeX macros v4.0.

Fig. 1.— Near-IR spectra of Hawaii 167. The upper spectrum was taken with the OH-airglow suppressor spectrograph while the lower one was taken with the CGS4 spectrometer. The thick lines show the fits to the Hα and the Hβ emission lines, using a gaussian and a linear continuum. The horizontal dash-dot lines indicate the broad-band magnitudes listed in Cowie et al. (1994b). Note the suggested detection of a 4000 Å break in the upper plot. The black solid circles indicate the flux of the fitted linear continuum at the central wavelengths of the J, H, and K' bands. These points are used in Figs. 3–5 as reference points when the observed spectra are compared with the models. The point at 4000 Å, which lies on the extension of the H-band continuum fit, is also used in the figures to see whether the models fit the possible 4000 Å break feature. Also, we conclude that the feature at $\sim$ 5007 Å is an instrumental artifact because its width is narrower than the instrumental profile.

Fig. 2.— Near-IR spectra of Q0059-2735. Both spectra were taken with the CGS4 spectrometer. The thick lines are the fits to Hα and Hβ. Two gaussians were used simultaneously for Hα to improve the fit. For Hβ, we mirror-reflected the left half of the line to the right and then fitted a gaussian, in order to avoid contamination from the Fe II emission lines clearly seen to the right. The horizontal dash-dot lines indicate the broad-band magnitudes listed in Cowie et al. (1994b). The black solid circles indicate the flux of the fitted linear continuum at the central wavelengths of the J and H bands. These points are used in Figs. 3 and 4 as reference points when the observed spectra are compared with the models.

Fig. 3.— (A) A flat spectrum ($f_\nu \propto \nu^{-1}$) simulating the QSO continuum for Hawaii 167; (B) The spectrum (A) reddened with the SMC extinction law and $E(B-V) = 0.08$; (C) A flat spectrum QSO continuum simulation as in (A), but for Q0059-2735. The squares and the triangles indicate the observed spectra for the two objects. These spectra were corrected for the foreground Galactic reddening by assuming $E(B-V) = 0.14$ for Hawaii 167 and $E(B-V) = 0.02$ for Q0059-2735. The vertical error bars indicate a conservative estimate of

30% photometric errors. The broad-band measurements from Cowie et al. (1994b) are shown as points with horizontal bars, whose lengths correspond to the band widths, while the points without horizontal bars are the reference points derived from our spectral measurements (black solid circles marked in Figs. 1 and 2). The optical spectrum of Hawaii 167, taken from Cowie et al. (1994b), is scaled so that it gives the correct I magnitude as listed in that paper. All reference SEDs (A, B, and C) are scaled such that they match the observed flux at the longest wavelength.

Fig. 4.— (A) A flat spectrum ($f_\nu \propto \nu^{-1}$) simulating the QSO continuum for Hawaii 167; (B) The spectrum (A) reddened with the SMC extinction law and $E(B-V) = 0.7$; (C) A flat spectrum QSO continuum simulation as in (A), but for Q0059-2735; (D) The spectrum (C) reddened with the SMC extinction law and $E(B-V) = 0.35$. An intrinsic Balmer decrement of 5 was assumed. The SEDs are scaled such that the reddened continuum matches the observed flux at Hα. All symbols are the same as for Fig. 3. The percentages below the two solid lines indicate the relative contributions of (B) and (D) to the observed spectra at the wavelengths of Mg II, Hβ, and Hα. In the case of Mg II in Q0059-2735, this value is with respect to the power-law line (C) in Fig. 3. The percentage (35%) just below the UV spectrum of Hawaii 167 indicates the amount of the observed UV light at 2000 Å with respect to the power-law continuum (A). Since the amount of the reddened light (B) at this wavelength is negligible, this is equal to the amount of scattered light.

Fig. 5.— (A) The Bruzual-Charlot instantaneous burst model with a Salpeter IMF ($0.1 < M < 125 M_\odot$), and age = 38 Myr; (B) Same as for (A) but with an age = 1 Gyr; (C) The estimated QSO continuum as for (B) in Fig. 4 but scaled by assuming the intrinsic Hβ equivalent width of 100 Å. (D) The model SED shown in (A) but with an age = 15 Myr; (E) the spectrum (D) reddened with the SMC extinction law and E(B–V)=0.23. The squares in the upper plot indicate the observed spectrum shown in Figs. 3 and 4 while the solid circles

show the spectrum after the subtraction of the QSO spectrum (C). The percentages indicate the contribution of (C) to the observed spectra at the wavelengths of Mg II, Hβ, and Hα.

Fig. 6.— Model E from Fig. 4 is compared with the observed near-IR spectrum of Hawaii 167 in Fig. 1 after correction of the observed spectrum for the Galactic reddening.

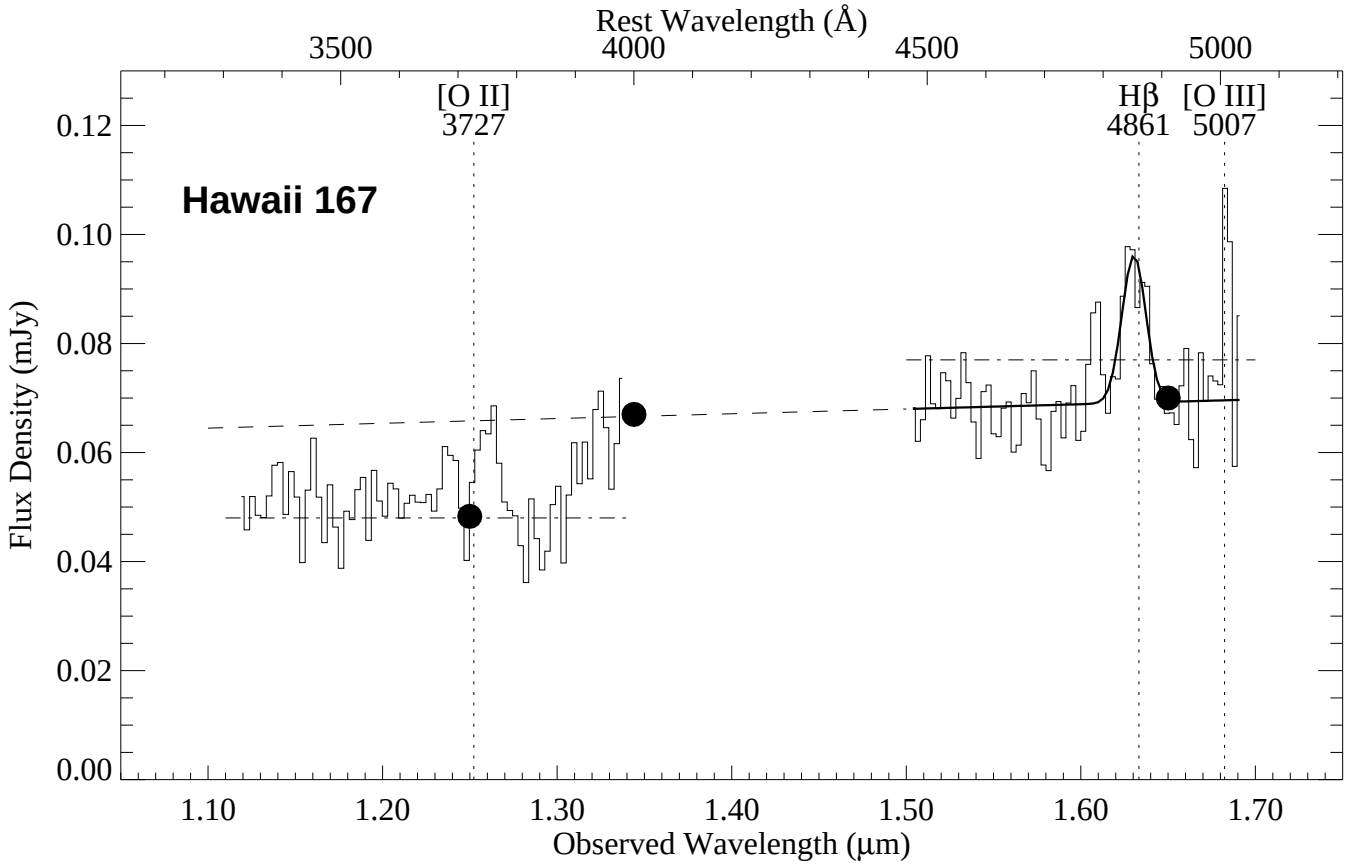
Rest Wavelength (Å)
3500
4000
4500
5000
[O II]
3727
Hβ
4861
[O III]
5007
Hawaii 167
0.12
0.10
0.08
0.06
0.04
0.02
0.00
Flux Density (mJy)
1.10
1.20
1.30
1.40
1.50
1.60
1.70
Observed Wavelength (μm)

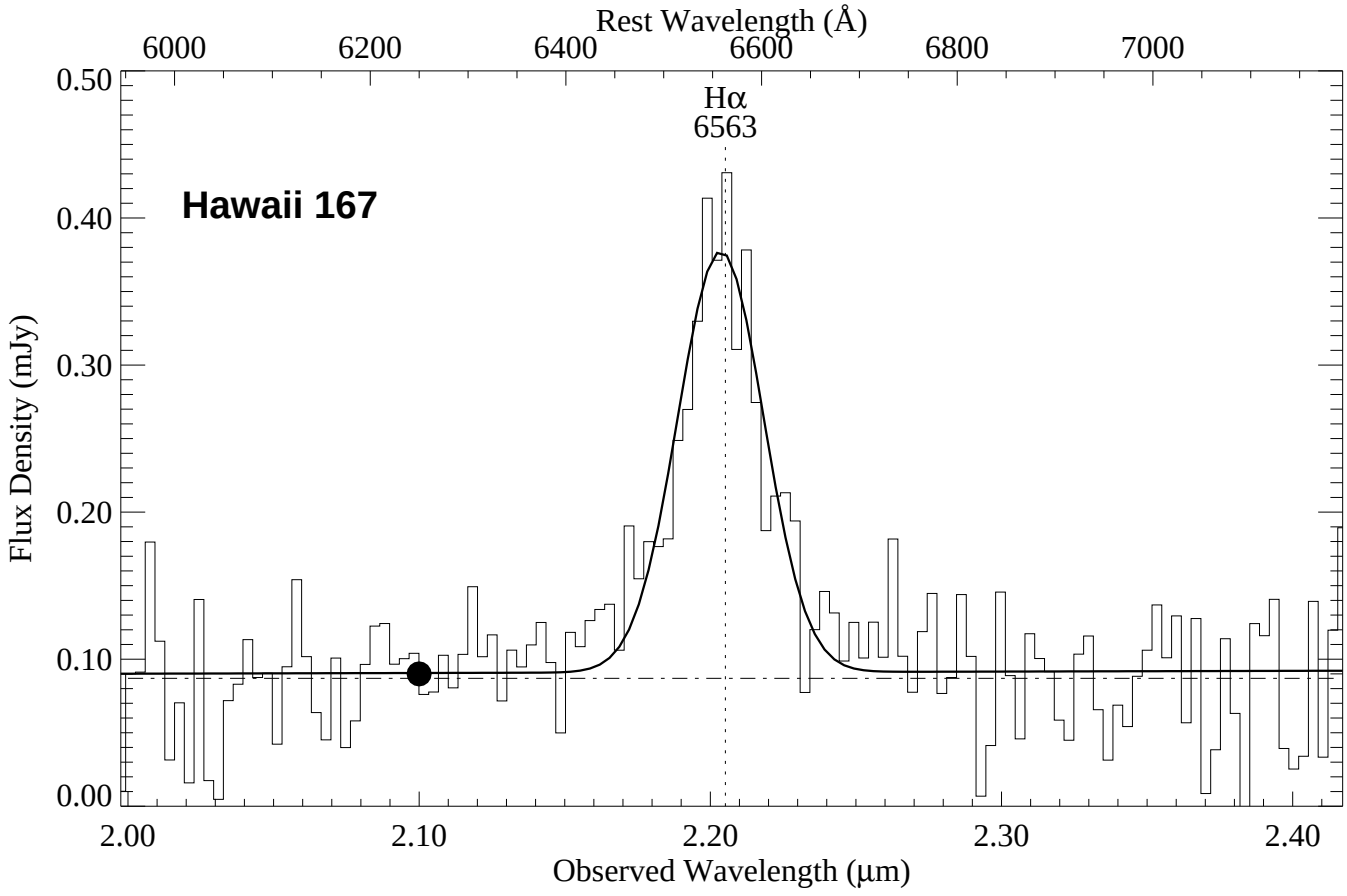
Rest Wavelength (Å)
6000
6200
6400
6600
6800
7000
Hα
6563
Hawaii 167
0.50
0.40
0.30
0.20
0.10
0.00
Flux Density (mJy)
2.00
2.10
2.20
2.30
2.40
Observed Wavelength (μm)

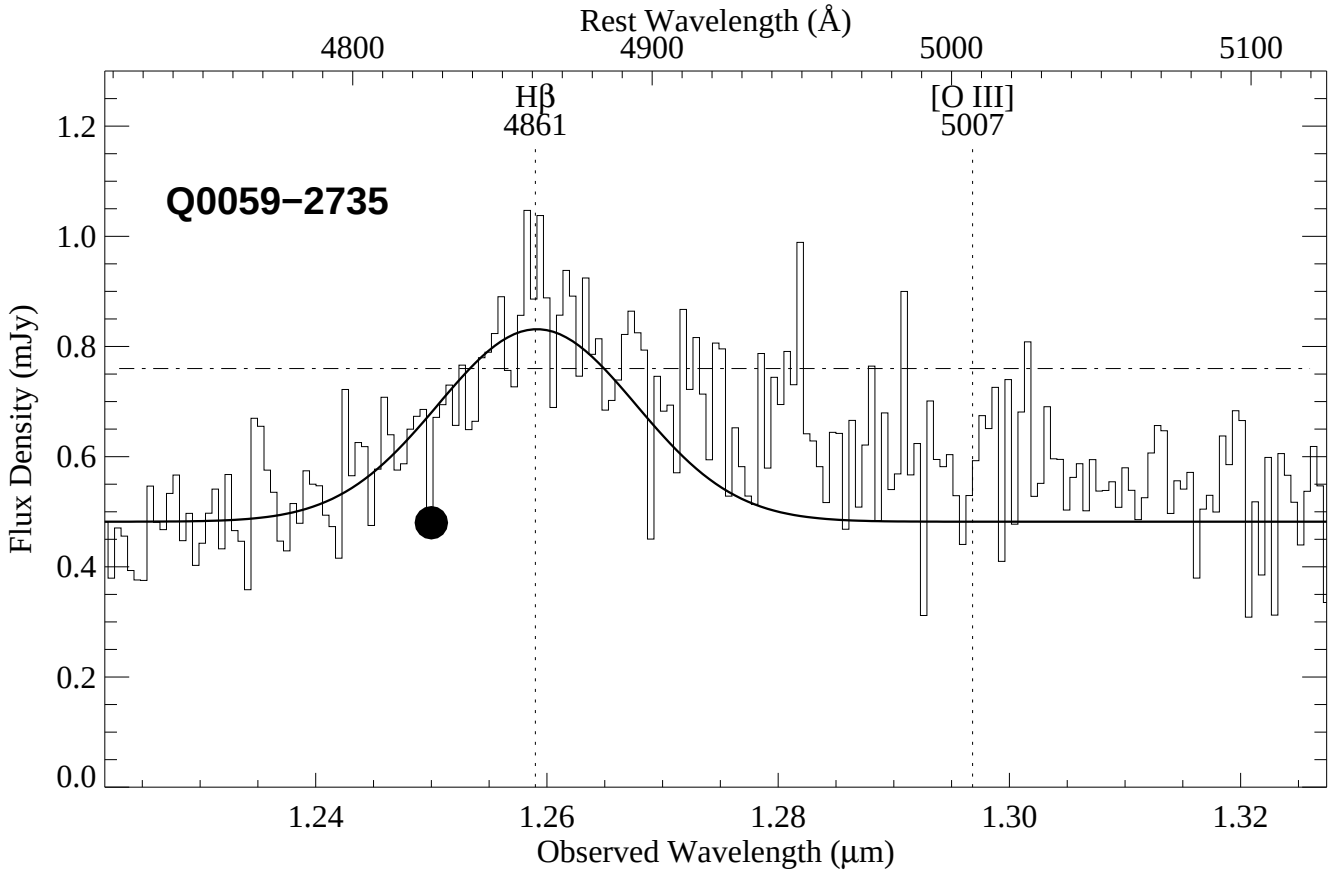
Rest Wavelength (Å)
4800
4900
5000
5100
Hβ
4861
[O III]
5007
Q0059−2735
Flux Density (mJy)
0.0
0.2
0.4
0.6
0.8
1.0
1.2
1.24
1.26
1.28
1.30
1.32
Observed Wavelength (μm)

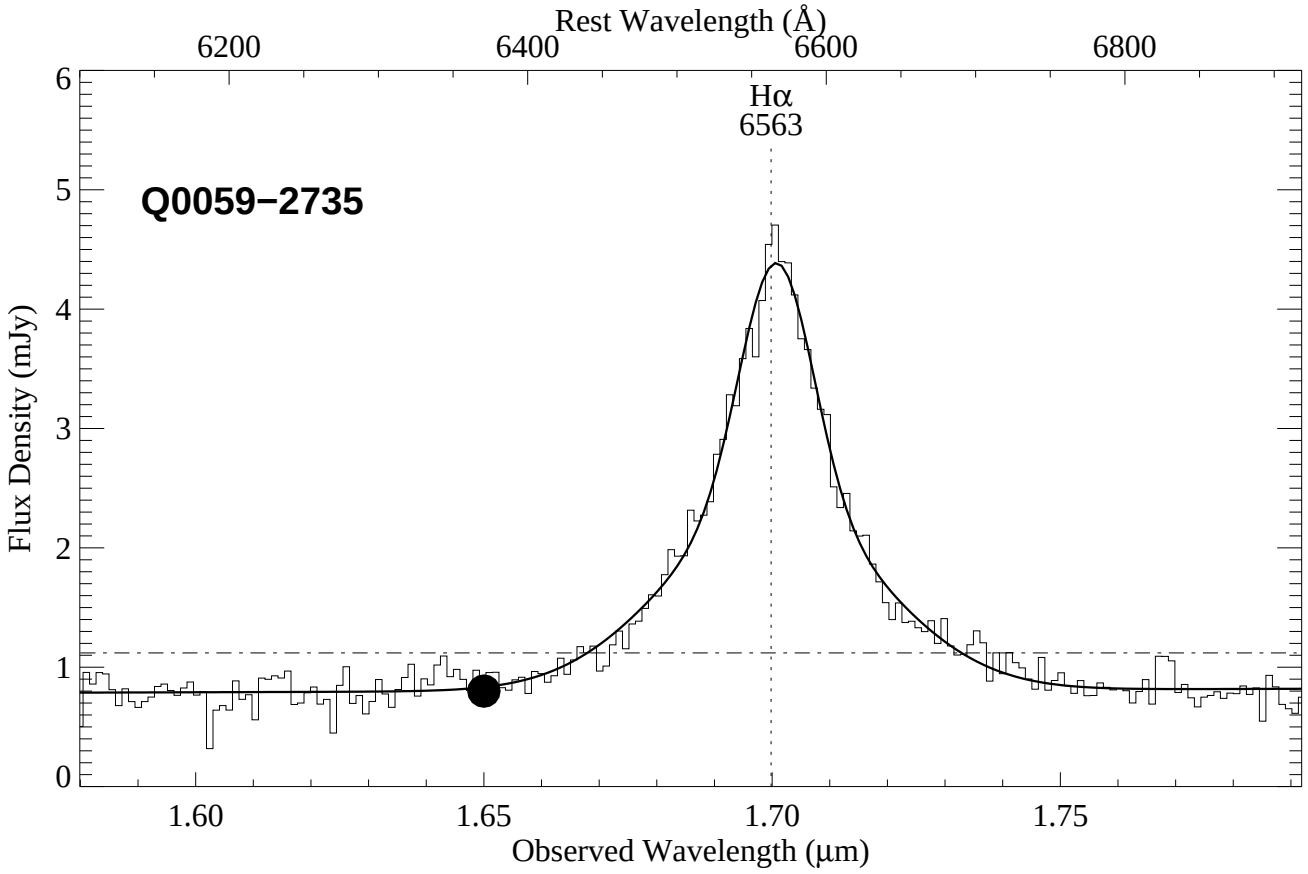
Rest Wavelength (Å)
6200
6400
6600
6800
Hα
6563
Q0059−2735
Flux Density (mJy)
0
1
2
3
4
5
6
1.60
1.65
1.70
1.75
Observed Wavelength (μm)

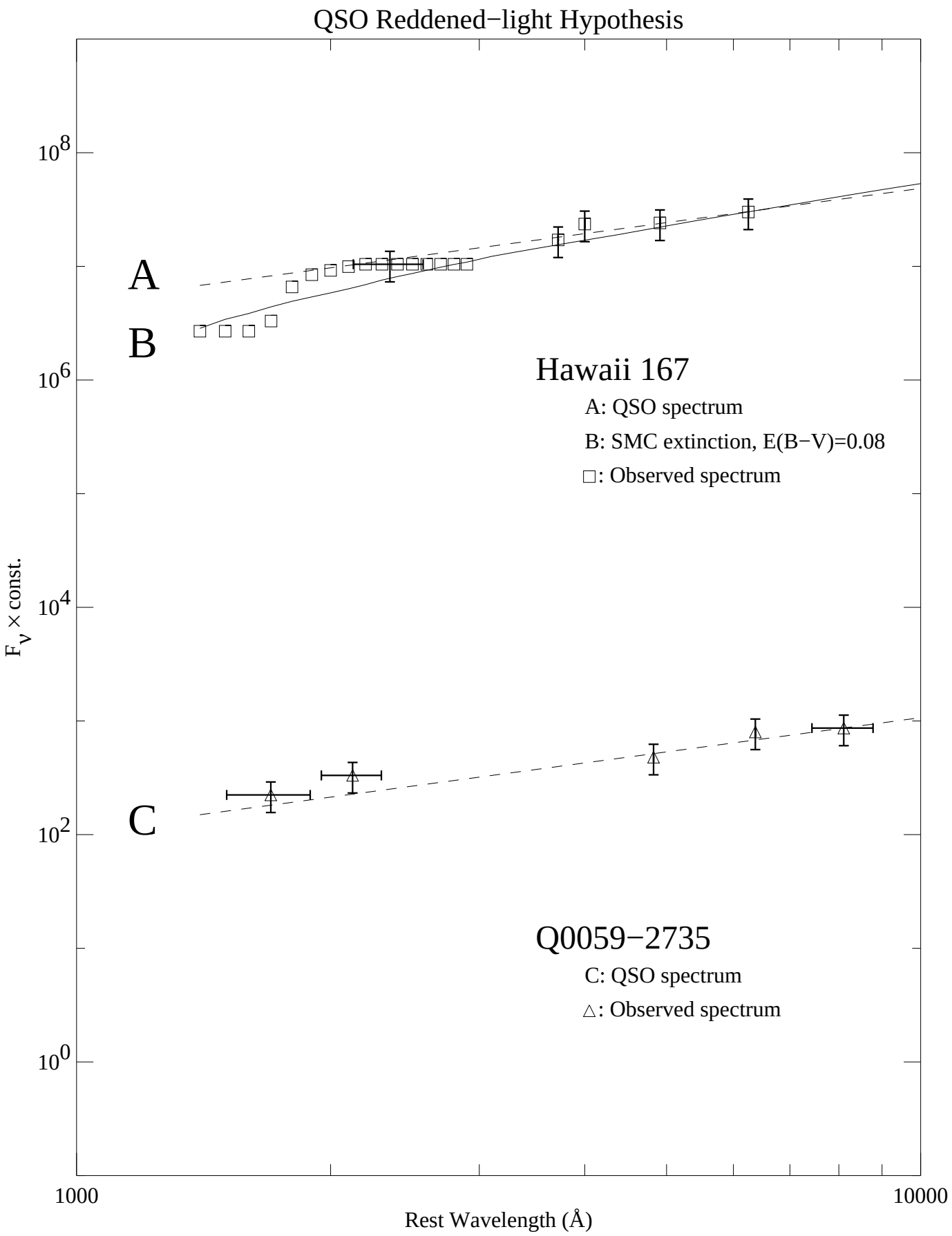
QSO Reddened−light Hypothesis
A
B
C
Hawaii 167
A: QSO spectrum
B: SMC extinction, E(B−V)=0.08
□: Observed spectrum
Q0059−2735
C: QSO spectrum
△: Observed spectrum
10^8
10^6
10^4
10^2
10^0
$F_\nu \times$ const.
1000
10000
Rest Wavelength (Å)

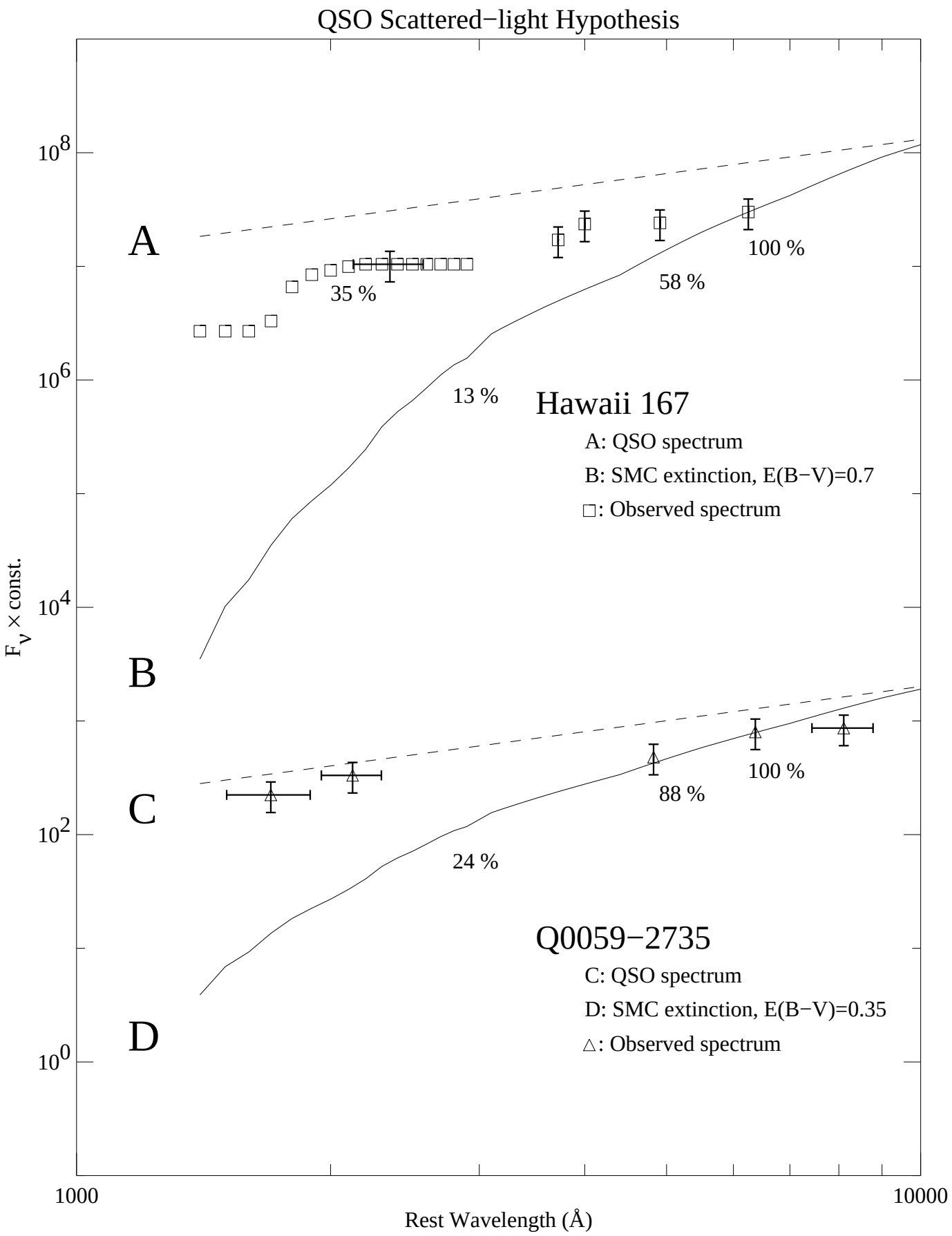
QSO Scattered−light Hypothesis
10^8
10^6
10^4
10^2
10^0
$F_\nu \times$ const.
A
B
C
D
35 %
58 %
100 %
13 %
88 %
100 %
24 %
Hawaii 167
A: QSO spectrum
B: SMC extinction, E(B−V)=0.7
□: Observed spectrum
Q0059−2735
C: QSO spectrum
D: SMC extinction, E(B−V)=0.35
△: Observed spectrum
1000
10000
Rest Wavelength (Å)

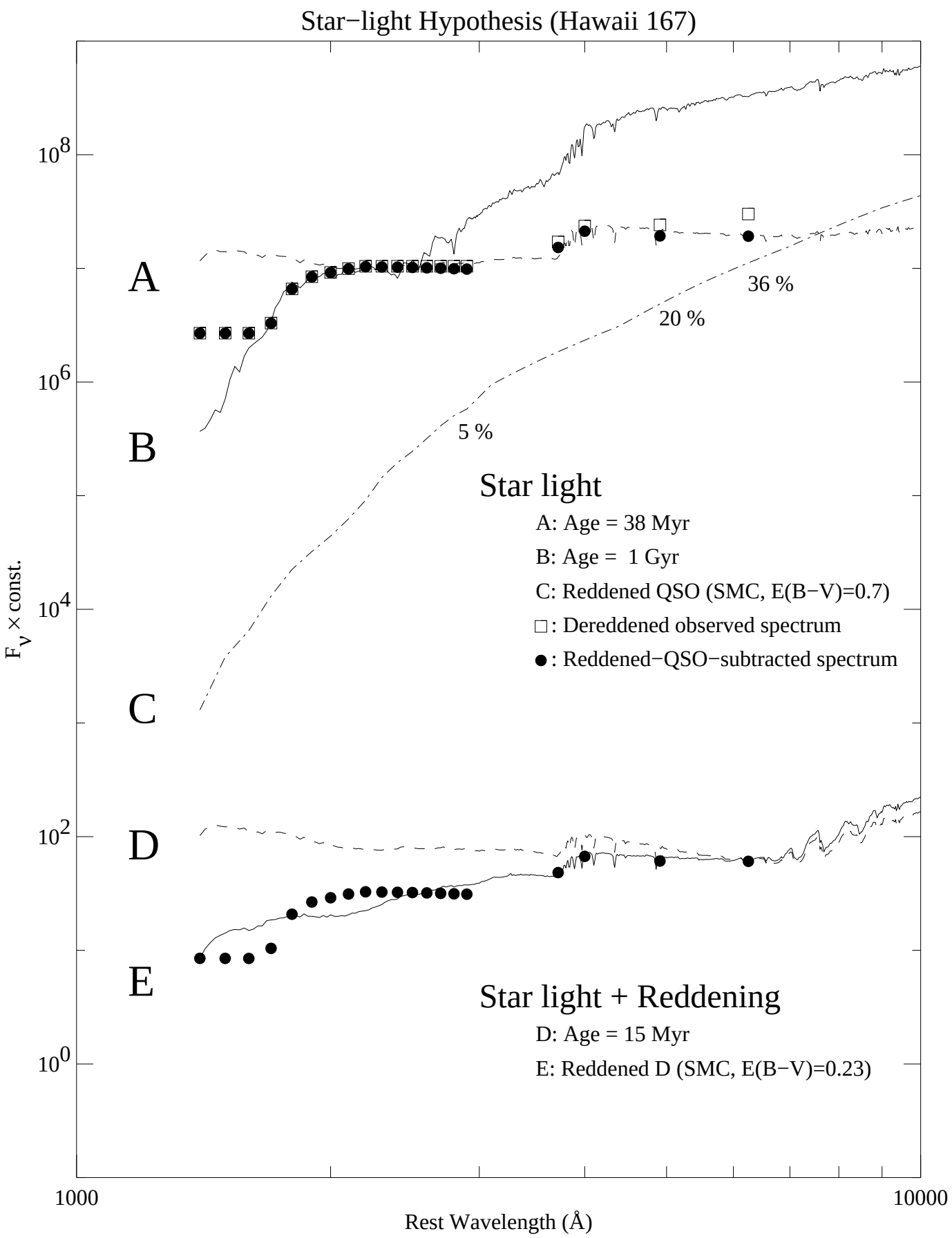
Star−light Hypothesis (Hawaii 167)
10^8
10^6
10^4
10^2
10^0
$F_\nu \times$ const.
A
B
C
D
E
36 %
20 %
5 %
Star light
A: Age = 38 Myr
B: Age = 1 Gyr
C: Reddened QSO (SMC, E(B−V)=0.7)
□: Dereddened observed spectrum
●: Reddened−QSO−subtracted spectrum
Star light + Reddening
D: Age = 15 Myr
E: Reddened D (SMC, E(B−V)=0.23)
1000
10000
Rest Wavelength (Å)

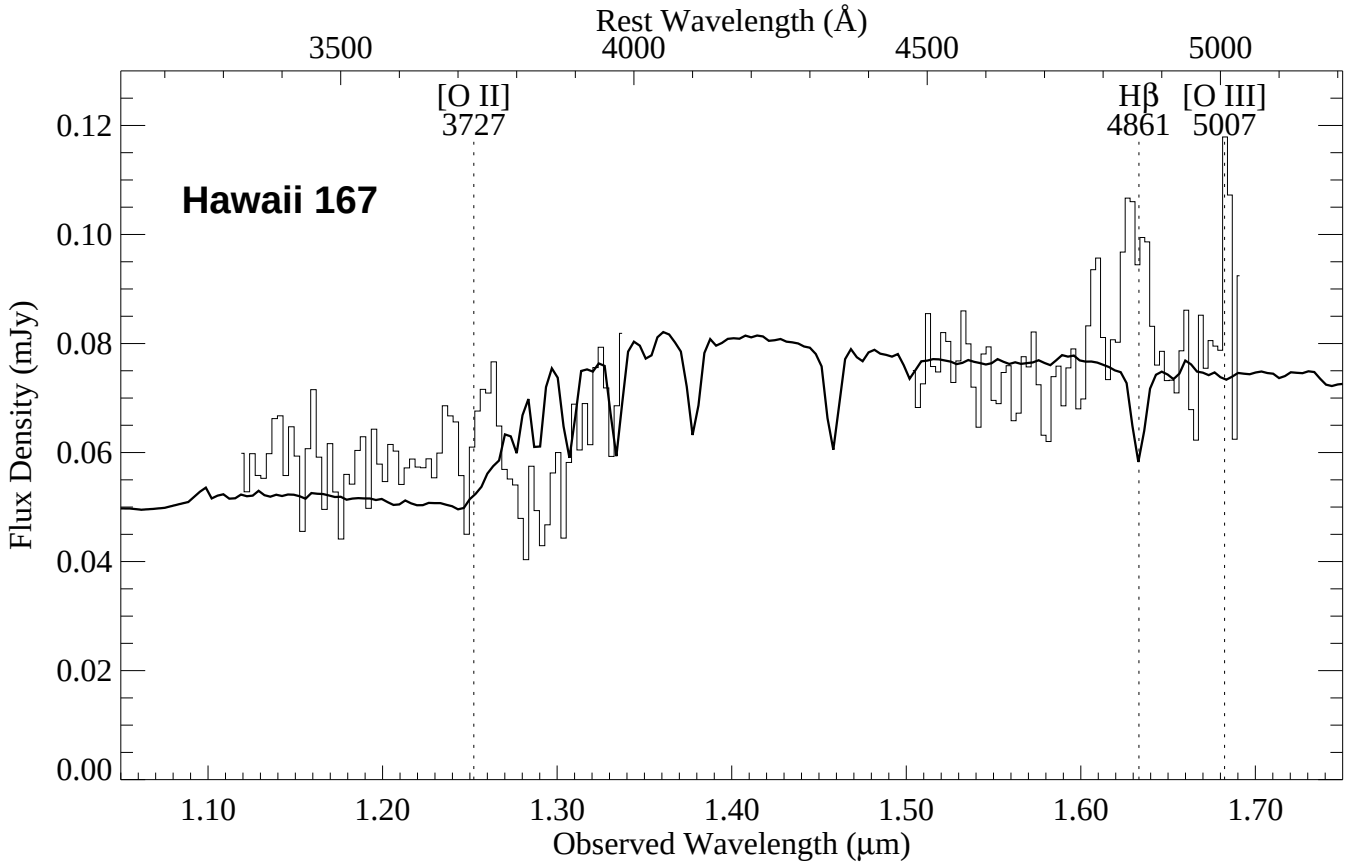
Rest Wavelength (Å)
3500
4000
4500
5000
[O II]
3727
Hβ
4861
[O III]
5007
Hawaii 167
0.12
0.10
0.08
0.06
0.04
0.02
0.00
Flux Density (mJy)
1.10
1.20
1.30
1.40
1.50
1.60
1.70
Observed Wavelength (μm)

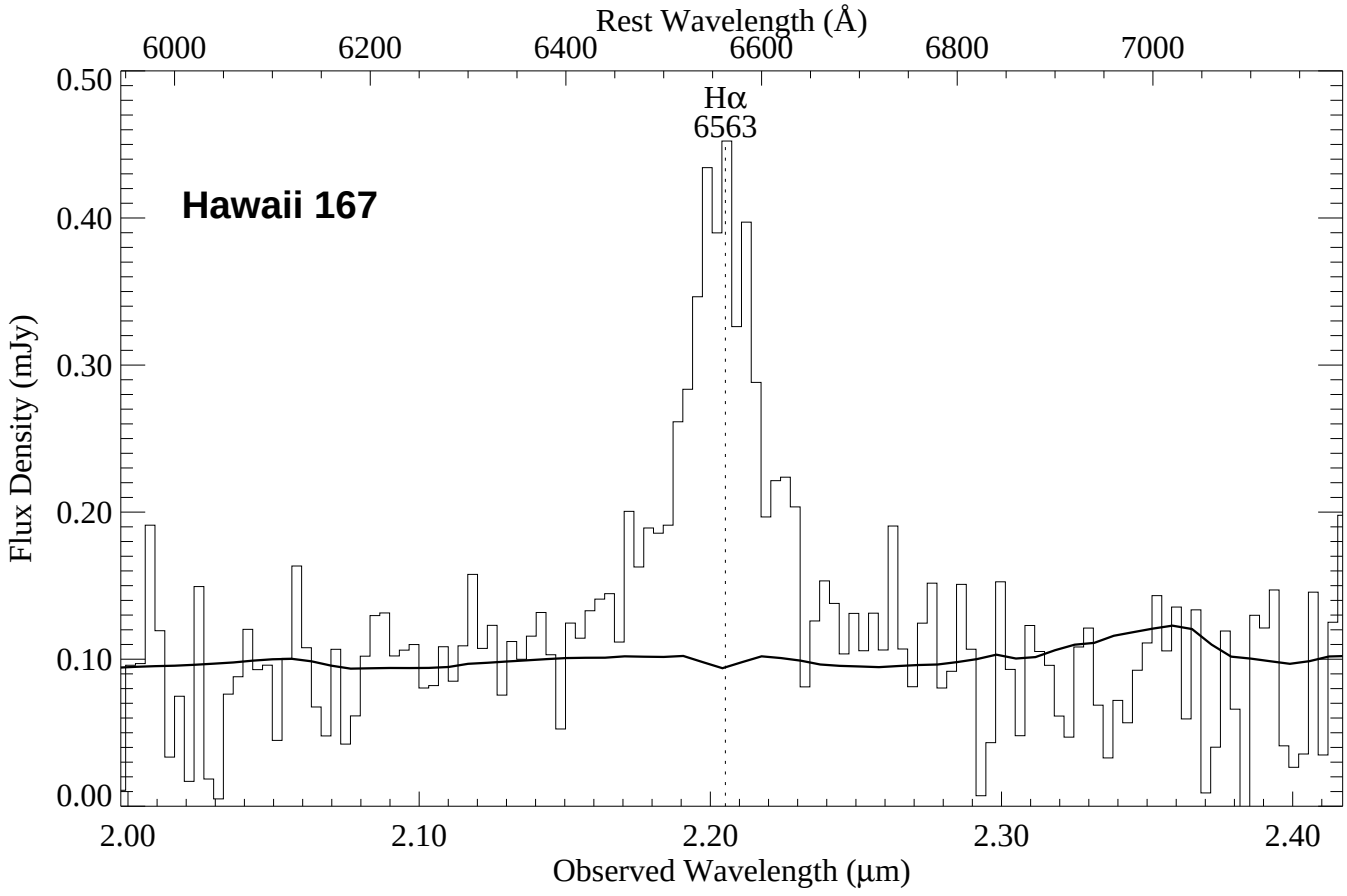
Rest Wavelength (Å)
6000
6200
6400
6600
6800
7000
Hα
6563
Hawaii 167
0.50
0.40
0.30
0.20
0.10
0.00
Flux Density (mJy)
2.00
2.10
2.20
2.30
2.40
Observed Wavelength (μm)

TABLE 1. Line Parameters

Object	Line	z	Continuum (mJy)	Peak (mJy)	FWHM (km s^{-1})	Line flux (W m^{-2})	EW[a] (Å)	Hα/Hβ
Q0059-2735	Hα	1.591	$8.0 \pm 0.1(-1)$	1.5 ± 0.1	7600 ± 400	$7.2 \pm 0.3(-17)$	$3.3 \pm 0.2(2)$	7.6 ± 0.9
		1.591		2.1 ± 0.1	2600 ± 200	$3.4 \pm 0.3(-17)$	$1.6 \pm 0.2(2)$	
	Hβ	1.590	$4.8 \pm 0.1(-1)$	$3.5 \pm 0.1(-1)$	4800 ± 400	$1.4 \pm 0.1(-17)$	$6.0 \pm 0.7(1)$	
Hawaii 167	Hα	2.358	$9.1 \pm 0.4(-2)$	$2.9 \pm 0.2(-1)$	4700 ± 300	$6.5 \pm 0.4(-18)$	$3.5 \pm 0.3(2)$	13 ± 3
	Hβ	2.354	$6.9 \pm 0.1(-2)$	$2.7 \pm 0.4(-2)$	2900 ± 600	$0.5 \pm 0.1(-18)$	$2.0 \pm 0.4(1)$	

[a]EW is corrected to the restframe value.